

## Triggered tremor sweet spots in Alaska

Joan Gomberg<sup>1</sup> and Stephanie Prejean<sup>2</sup>

Received 8 April 2013; revised 5 November 2013; accepted 12 November 2013; published 16 December 2013.

[1] To better understand what controls fault slip along plate boundaries, we have exploited the abundance of seismic and geodetic data available from the richly varied tectonic environments composing Alaska. A search for tremor triggered by 11 large earthquakes throughout all of seismically monitored Alaska reveals two tremor “sweet spots”—regions where large-amplitude seismic waves repeatedly triggered tremor between 2006 and 2012. The two sweet spots locate in very different tectonic environments—one just trenchward and between the Aleutian islands of Unalaska and Akutan and the other in central mainland Alaska. The Unalaska/Akutan spot corroborates previous evidence that the region is ripe for tremor, perhaps because it is located where plate-interface frictional properties transition between stick-slip and stably sliding in both the dip direction and laterally. The mainland sweet spot coincides with a region of complex and uncertain plate interactions, and where no slow slip events or major crustal faults have been noted previously. Analyses showed that larger triggering wave amplitudes, and perhaps lower frequencies ( $< \sim 0.03$  Hz), may enhance the probability of triggering tremor. However, neither the maximum amplitude in the time domain or in a particular frequency band, nor the geometric relationship of the wavefield to the tremor source faults alone ensures a high probability of triggering. Triggered tremor at the two sweet spots also does not occur during slow slip events visually detectable in GPS data, although slow slip below the detection threshold may have facilitated tremor triggering.

**Citation:** Gomberg, J., and S. Prejean (2013), Triggered tremor sweet spots in Alaska, *J. Geophys. Res. Solid Earth*, 118, 6203–6218, doi:10.1002/2013JB010273.

### 1. Introduction

[2] Studies of seismic tremor provide new constraints on the processes governing fault slip [see Obara, 2002; Rogers and Dragert, 2003; Gomberg, 2010; Peng and Gomberg, 2010; Rubinstein et al., 2009; Vidale and Houston, 2012, and references therein]. In particular, tremor and geodetically observed slow slip measurements provide constraints on sections of faults that were previously largely inaccessible to observation. Slow slip describes transient, shear displacements across fault surfaces that develop too slowly to generate typical earthquakes. The seismic manifestations of slow slip are thought to arise from rapid failure of tiny, weak, asperities as the slow slip front passes, mostly apparent as “tremor.” Ambient tremor appears as low-amplitude, emergent bursts of seismic energy in the 1–10 Hz passband, lasting from tens of minutes to hours, which are coherent across multiple sites separated by tens of kilometers. Tremor activity levels wax

and wane, apparently as slow slip fronts pass over and subside [Ando et al., 2010; Wech and Creager, 2011; Ghosh et al., 2012]. Triggered tremor refers to signals similar to ambient tremor that arrive during the passage of seismic waves that originate elsewhere, and is seen as shorter bursts that repeat roughly in step with the period of the passing waves [Gomberg, 2010]. While slow slip may be observed more directly using geodetic data, tremor observations serve as much higher resolution proxies [Obara et al., 2004; Aguiar et al., 2009].

[3] Tremor and slow slip have been studied now in many of the world’s subduction zones and along a few transform plate boundaries, with Alaska (mainland Alaska and most of the Aleutian arc) among the most recent subduction zones where tremor has been observed [Ohta et al., 2006; Peterson and Christensen, 2009; Brown et al., 2013]. Slow slip and tremor studies in the Alaskan subduction zone have the great benefit of sampling a diversity of environments along its  $\sim 4000$  km span (Figure 1). Mainland Alaska has been shaped by continental-oceanic plate interactions with motions and boundaries that transition westward from transform to obliquely convergent. The coastal regions of easternmost Alaska parallel the transform Fairweather-Queen Charlotte boundary between the Pacific and North American plates until  $\sim 58^\circ\text{N}$ . From there and south of the Denali Fault Zone, plate interactions become particularly complex, owing to the transport and accretion of various oceanic and arc terranes to the North American plate, of which the Yakutat

<sup>1</sup>U.S. Geological Survey, Department of Earth and Space Sciences, University of Washington, Seattle, Washington, USA.

<sup>2</sup>Alaska Science Center, U.S. Geological Survey, Anchorage, Alaska, USA.

Corresponding author: J. Gomberg, U.S. Geological Survey, Department of Earth and Space Sciences, University of Washington, PO Box 351310, Seattle, WA 98195-1310, USA. (gomberg@usgs.gov)

©2013. American Geophysical Union. All Rights Reserved.  
2169-9313/13/10.1002/2013JB010273

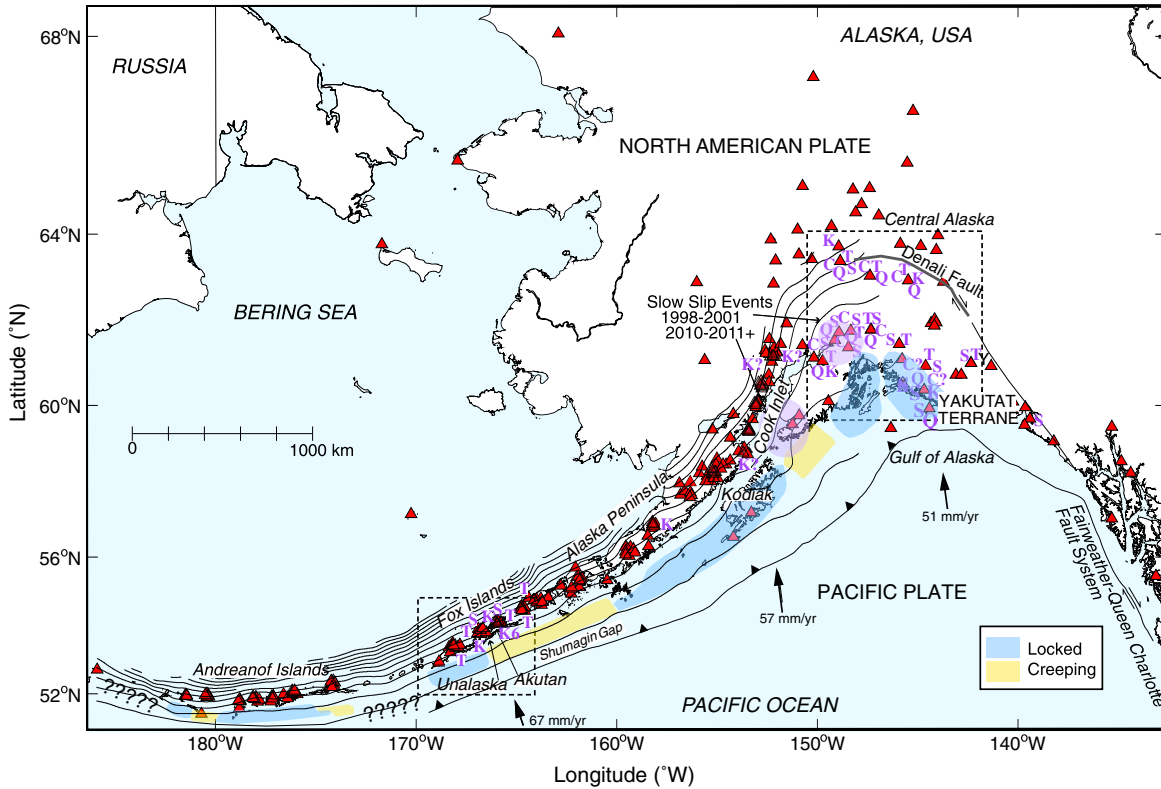


**Figure 1.** Map of Alaska. The Denali Fault is part of the transform boundary that extends southeasterly to the Gulf of Alaska, between the northwesterly converging North American and Pacific plates. Elsewhere, the Pacific plate is subducting (boundary shown by the hachured line). Locations of seismic stations that provided data examined in this study shown as triangles. Depths to the plate interface are contoured at 20 km intervals [from Hayes *et al.*, 2012] starting at the trench (hachured curve) and the generalized plate-coupling model (blue and yellow shading) of Freymueller *et al.* [2008] and patches where slow slip occurred (purple areas) in 1998–2001 [Ohta *et al.*, 2006] and from 2010 until at least 2011 [Wei *et al.*, 2012] are shown. Purple letters atop seismic stations indicate tremor was observed, triggered by the Queen Charlotte (Q), *M*8.6 Sumatra (S), Chile (C), Tohoku (T), 2007 Kuril Islands (K or K?), and 2006 Kuril Islands (K6) earthquakes. Dashed boxes outline larger-scale mapped regions in Figures 4 and 5.

terrane is the most recent. The Yakutat terrane is an oceanic plateau mostly composed of anomalously thick and buoyant oceanic crust [Worthington *et al.*, 2012]. Various deformation modes accommodate its collision, from crustal folds and thrusts that shallow into a décollement atop the Yakutat basement transitioning westward to subduction of Yakutat terrane (see section 6 for more details) [Eberhart-Phillips *et al.*, 2006; Koons *et al.*, 2010; Worthington *et al.*, 2012; Elliott *et al.*, 2013]. Beyond the continental margin at the western limit of the Alaska Peninsula, steeply dipping, oceanic-oceanic plate subduction that changes from trench-normal to significantly oblique going westward produces the Aleutian arc. From east to west across this entire system the age and convergent rate of the Pacific plate increase, from ~35 to ~63 Ma and 5.1 to 7.5 cm/yr, respectively [DeMets *et al.*, 1994; Freymueller *et al.*, 2008; Ruppert *et al.*, 2008]. In addition, the degree to which the plate interface is coupled, measured as the difference between the long-term convergence rate and average slip rate between major interplate earthquakes (slip deficit), varies spatially both along strike and dip and probably temporally as well [Freymueller *et al.*, 2008; Freymueller, 2012].

[4] Much of Alaska has been monitored seismically, potentially permitting examination of the relationship between tremor production and the varying local geologic environments (Figure 1). Only one study has examined ambient tremor in mainland Alaska, along a transect extending several hundred kilometers from Cook Inlet, using several months of data from a temporary 1998–2001 seismic network deployment augmented by seismograms from the permanent Alaska Earthquake Information Center (AEIC) seismic network [Peterson and Christensen, 2009]. Peterson and Christensen [2009] found tremor that originated near the downdip edge of a concurrent slow slip event [Ohta *et al.*, 2006]. Another study that employed continuous data from the AEIC and a temporary seismic network in a systematic search for tremor tested and rejected the hypothesis that tremor should accompany afterslip following the 2002 *M*7.9 Denali Fault earthquake [Gomberg *et al.*, 2012]. Brown *et al.* [2013] searched for ambient tremor and low-frequency earthquakes (LFEs) in data recorded between 2005 and 2011 on Alaska Volcano Observatory (AVO) networks deployed on many Aleutian Islands and surrounding mainland volcanoes. The AVO networks are operated for the purpose of volcano monitoring. Brown *et al.* [2013] also used

**Table 1.** Candidate Triggering Earthquake Information<sup>a</sup>

Earthquake	$M$	Latitude	Longitude	Depth (km)	Origin Time	Unalaska/Akutan Tremor	Mainland Tremor
Queen Charlotte	7.7	52.781	-132.103	20	10/28/12 3:4:9	N	Y
Andreanof Islands	6.4	51.634	178.293	10	9/26/12 23:39:54	?	N
Sumatra	8.2	0.773	92.452	16	4/11/12 10:43:09	N	N
Sumatra	8.6	2.311	93.063	23	4/11/12 08:38:37	Y	N
Fox Islands	7.2	52.008	-171.859	63	6/24/11 03:09:40	?	N
Tohoku	9.0	38.30	142.37	29	3/11/11 05:46:24	Y	Y
Chile	8.8	-36.12	-72.90	22	2/27/10 06:34:11	N	Y
Samoa	8.1	-15.49	-172.10	18	9/29/09 17:48:11	N	N
Kuril Islands	7.4	46.86	155.15	36	1/15/09 17:49:39	N	N
Kuril Islands	8.1	46.24	154.52	10	01/13/07 04:23:21	Y	Y
Kuril Islands	8.3	46.59	153.27	10	11/15/06 11:14:13	Y	N

<sup>a</sup>Each column lists parameters describing the earthquakes that generated candidate triggering waves for this study. Each row lists the name of the earthquake (column 1), its moment magnitude (column 2), the latitude, longitude, and depth of its hypocenter (columns 3–5), and the origin date and time (column 6). A “Y,” “N,” or “?” indicates that tremor was, was not, or may have been triggered near the Unalaska/Akutan (column 7) or mainland (column 8) sweet spot by the earthquake’s waves. Dates are presented as month/day/year.

AEIC data but focused on regions where tremor-like signals had been identified during daily routine visual scanning of AVO data for volcano monitoring and therefore looked mostly near AVO network sites along the Aleutian chain and the Alaska Peninsula. *Peterson et al.* [2011] also searched the same database and region but for the period 2005–2008. *Brown et al.* [2013] located LFE sources in four regions, near Kodiak Island, the Shumagin Gap, and the Unalaska and Andreanof Islands (Figure 1). *Peterson et al.* [2011] identified 12 tremor bursts in basically the same regions as in the *Brown et al.* [2013] study.

[5] The limited scope of the aforementioned studies largely reflects the daunting task of analyzing hundreds of continuous data streams in search of typically subtle tremor signals and in Alaska amidst frequently high noise levels, numerous earthquake signals, and possibly volcanic tremor [*D’Alessandro and Ruppert*, 2012]. To make a systematic search of all available continuous seismic data from throughout Alaska tractable, we focused on triggered tremor. In addition to limiting the time intervals examined to those spanning the passage of large-amplitude seismic waves, recordings of these waves provide precise measures of candidate triggering deformations [*Gomberg*, 2010; *Hill*, 2010, 2012a, 2012b]. We examined the tremor response to 11 large-amplitude seismic wavefields since 2006, selected for reasons described in section 2, using all available data recorded by the AVO, AEIC, and the Alaska and Pacific Tsunami Warning Center (ATWC) network stations (Table 1). We found multiple examples of clear triggered tremor signals only at sites on adjacent islands of Unalaska, Akutan and a few others, and surprisingly at a set of sites in central, mainland Alaska. The prevalence of tremor in this region of the Aleutians was expected, noting that *Brown et al.* [2013] showed a total tremor duration in the vicinity of Unalaska/Akutan almost double that in any of the other regions examined. This Unalaska/Akutan tremor “sweet spot” also is consistent with anecdotal evidence in the AVO daily activity logs, in which analysts most often note nonvolcanic tremor-like signals at these same stations. The mainland sweet spot is located well south of the Denali Fault and not near any other mapped crustal faults. Its location relative to the boundary of the subducted Yakutat slab inferred by *Eberhart-Phillips et al.* [2006], the areal extent of the coupled Yakutat terrane inferred in *Elliott et al.* [2013] and the relative lack of earthquake activity in the sweet spot region makes it consistent with models in which tremor serves as a proxy for slow slip along an interface with frictional properties transitional

between stable and stick-slip responses to tectonic loading. However, no geodetically identified slow slip events have been documented nearby or coincident with the mainland sweet spot.

[6] In this paper we first summarize the results of our search for tremor within 11 large-amplitude seismic wavetrains. In section 3 on triggered tremor observations, we show estimates of the epicenters of some of the tremor sources. We then describe the characteristics of the 11 triggering wavefields that might facilitate tremor generation (section 4). We find imperfect correlations with peak triggering wave amplitudes and other characteristics and the observation of triggered tremor. This, and the established association of tremor with slow slip led us to look for evidence of slow slip in GPS data, presented in section 5. In section 6, we offer some interpretation of the temporal and spatial extents of the two tremor sweet spots in the context of the geology and tectonics of Alaska and slow slip phenomena generally.

## 2. Data

[7] We focused our study on the period 2006 and later, commensurate with when the AVO’s monitoring capabilities became adequate for our analyses. Our goal was to examine the response to candidate triggering waves with a range of amplitudes, durations, and frequencies. We note that achieving this goal does not require a complete sampling of all wavefields exceeding some posited threshold. Thus, we employed some simple search criteria that would identify earthquakes likely to have sent waves across Alaska with amplitudes potentially large enough to trigger (based on previous studies elsewhere), with a range of durations and frequencies (i.e. sources at varying distances). For our initial search we considered all  $M > 7.0$  earthquakes in Japan, the Kuril and Aleutian Islands, and near mainland Alaska, as well as all  $M > 8$  earthquakes globally. A preliminary scan of data archived at the AVO showed data were either unavailable or inadequate for quite a few of these events (e.g., had poor signal-to-noise ratios and/or data gaps). This left 11 candidate triggering earthquakes that sent large and well-recorded waves across Alaska (Table 1).

[8] For each of the 11 candidate triggering earthquake wavefields, we requested from the IRIS (Incorporated Research Institutions for Seismology) Data Management Center all short and long period, high gain seismograms from the AVO, AEIC, and ATWC networks. It is important

**Table 2.** Candidate Triggering Parameters at Unalaska/Akutan Sweet Spot (Station AKRB)<sup>a</sup>

Earthquake	Peak Velocity <i>Z</i>	Peak Velocity Radial	Peak Velocity Tangential	Back Azimuth	Days Since Last Tremor	Akutan Tremor
2012 Queen Charlotte	0.097	0.112	<i>0.193</i>	80	201	N
2012 Andreanof Islands	0.049	0.060	<i>0.077</i>	262	169	?
2012 <i>M</i> 8.2 Sumatra	0.020	0.029	<i>0.037</i>	280	0	N
2012 <i>M</i> 8.6 Sumatra	0.035	0.044	<i>0.051</i>	280	398	Y
2011 Fox Islands	0.364	<i>0.533</i>	<i>0.506</i>	241	293	?
2011 Tohoku	0.181	0.143	<i>0.265</i>	267	1519	Y
2010 Chile	<i>0.035</i>	0.034	0.033	111	1142	N
2009 Samoa	0.033	<i>0.068</i>	0.041	186	991	N
2009 Kuril Islands	0.042	0.048	<i>0.072</i>	269	734	N
2007 Kuril Islands	0.300	0.309	<i>0.372</i>	269	60	Y
2006 Kuril Islands	0.082	0.084	<i>0.127</i>	270	?	Y

<sup>a</sup>For each earthquake that generated candidate triggering waves that passed across the Unalaska/Akutan region (each row), this table lists the name of the earthquake (column 1, Table 1), peak velocities (cm/s) of the vertical (*Z*) and rotated horizontal components (columns 2–4), and the back azimuths from the recording station to the earthquake’s epicenter in degrees clockwise from the north (column 5) and the number of days since the previous triggered tremor detection (column 6). In each row, a “Y,” “N,” or “?” in the rightmost column indicates that tremor was, was not, or may have been triggered near the Unalaska/Akutan sweet spot by the earthquake waves. Amplitude and back azimuth information was measured on station AKRB. Maximum peak velocities among the three components are denoted by italicized values.

to note that characterization of the tremor response is affected by not only the station coverage (Figure 1) but also by highly variable noise levels, interference from other natural seismic sources, and data reporting. The earthquake “magnitude of completeness” ( $M_c$ ) provides a measure of the probability of observing tremor at all;  $M_c$  is the magnitude above which all earthquakes are reported in a catalog. Other studies and qualitative assessments in this study suggest that maximum tremor amplitudes are likely comparable to those from local  $M \sim 1.5$  earthquakes [see *Gomberg et al.*, 2012, and references therein]. A study of AEIC earthquake detection showed that for Alaska the lowest  $M_c$  is  $\sim 1.4$  in central mainland Alaska and is  $\sim 2.0 < M_c < \sim 2.6$  along the Alaska Peninsula and the Aleutians with the higher values where station density is sparser [*D’Alessandro and Ruppert*, 2012]. The AVO also produces a catalog of earthquakes that in the vicinity of the well-monitored volcanoes probably has a completion magnitude of  $M_c \sim 0.5$  [*Dixon et al.*, 2013]. We conclude that we could be failing to detect some tremor in some regions and can only confidently say where it does occur. In addition to the emergent low-amplitude wave trains that typify most tremor signals (often only envelopes are coherent

across multiple stations) [*Peng and Gomberg*, 2010], energy in the tremor passband from the triggering source sometimes arrives concurrently with triggered tremor signals for some large regional earthquakes.

[9] All seismic data used are ground velocities, recorded at 50 or 100 Hz. Many of the AVO stations consist of a single vertical (*Z*) component, short-period seismograph, and most mainland stations have three-component, broadband seismographs. For our tremor exploration, we manually scanned record sections of E-W components if available and the vertical components otherwise, after first filtering in both 2–10 Hz and  $>5$  Hz passbands. We checked for tremor bursts that appeared modulated by the surface waves radiated by the triggering earthquake, by displaying both filtered and unfiltered seismograms during scanning. To check for coherency of multiple modulated bursts across stations, we ordered seismograms according to station longitudes, which for most of Alaska conveniently arranged data from adjacent or nearby sites together. We required coherency at three or more stations and preferably subnetworks on adjacent islands. The exception to this is in central mainland Alaska, where ordering was set manually based on mapped station locations.

**Table 3.** Candidate Triggering Parameters at Mainland Sweet Spot (Station PAX)<sup>a</sup>

Earthquake	Peak Velocity <i>Z</i>	Peak Velocity Radial	Peak Velocity Tangential	Back Azimuth	Days Since Last Tremor	Mainland Tremor
2012 Queen Charlotte	0.049	<i>0.282</i>	0.216	139	201	Y
2012 Andreanof Islands	0.001	<i>0.010</i>	0.008	256	169	N
2012 <i>M</i> 8.2 Sumatra	0.006	0.057	<i>0.070</i>	300	0	N
2012 <i>M</i> 8.6 Sumatra	0.010	0.071	<i>0.120</i>	300	398	Y
2011 Fox Islands	0.005	0.031	<i>0.035</i>	244	293	N
2011 Tohoku	0.014	<i>0.095</i>	0.092	275	1519	Y
2010 Chile	0.007	<i>0.048</i>	0.046	122	1142	Y
2009 Samoa	0.005	<i>0.025</i>	0.020	206	991	N
2009 Kuril Islands	0.003	<i>0.022</i>	0.016	272	734	N
2007 Kuril Islands	0.016	0.079	<i>0.206</i>	272	?	Y
2006 Kuril Islands	0.014	<i>0.092</i>	0.073	273	?	N

<sup>a</sup>For each earthquake that generated candidate triggering waves that passed across the mainland sweet spot region (each row), this table lists the name of the earthquake (column 1, Table 1), peak velocities (cm/s) of the vertical (*Z*) and rotated horizontal components (columns 2–4), and the back azimuths from the recording station to the earthquake’s epicenter in degrees clockwise from the north (column 5) and the number of days since the previous triggered tremor detection (column 6). In each row, a “Y” or “N” in the rightmost column indicates that tremor was or was not triggered near the mainland sweet spot by the earthquake’s waves. Amplitude and back azimuth information was measured on station PAX. Maximum peak velocities among the three components are denoted by italicized values.

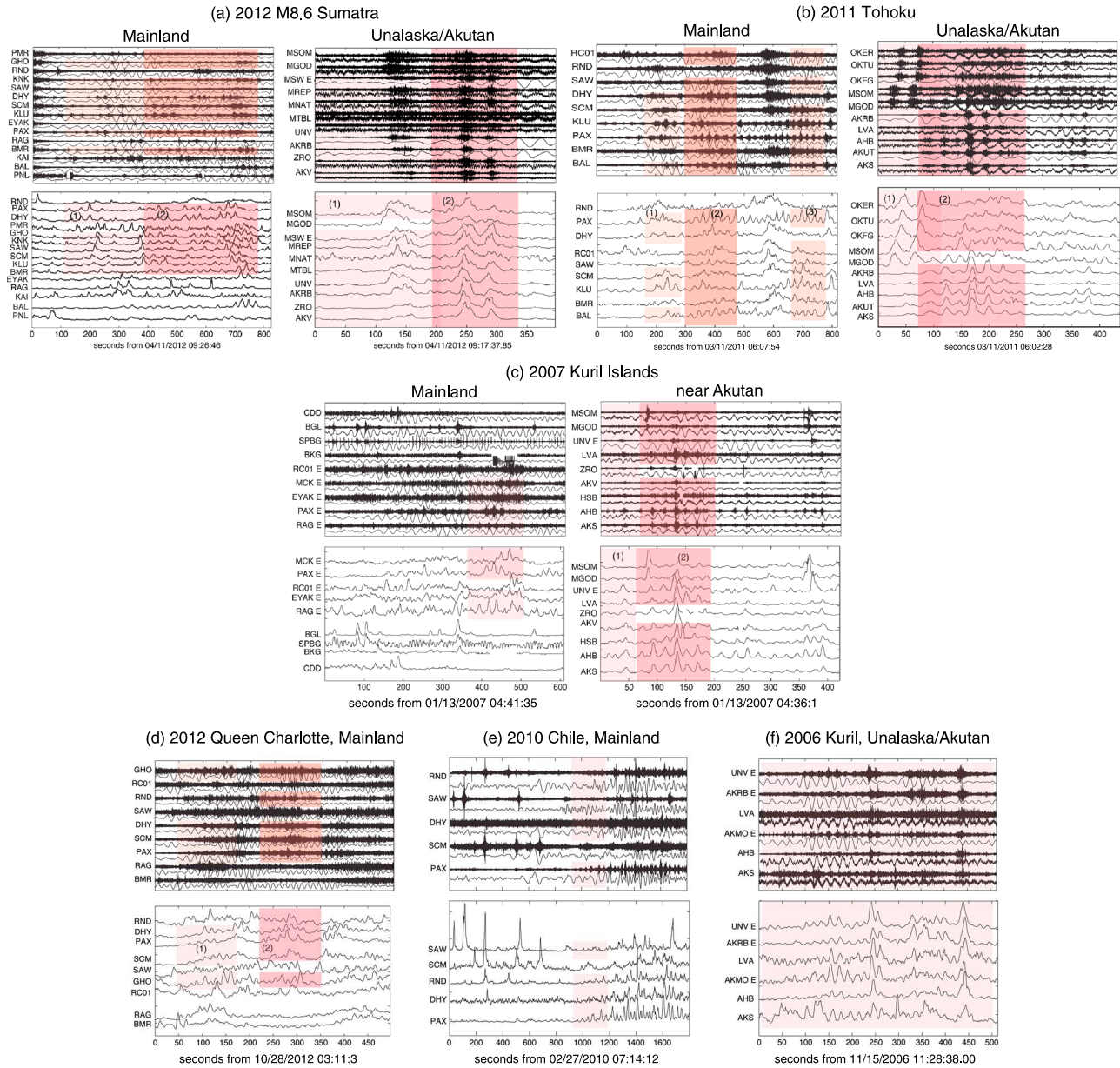


**Figure 2.** Record sections of triggered tremor waveforms and envelopes. (top) For each triggering earthquake, record sections of recorded and filtered waveforms (bottom and top traces, respectively) with triggered signals in longitudinal order, and (bottom) smoothed (5 s moving average) envelopes of the filtered waveforms ordered to maximize visually the coherence between envelopes. Recording stations are labeled on the left of each seismogram. If no component is noted, data are vertical components and an “E” indicates E-W motion. Filter passbands, chosen subjectively, generally are 2–10 Hz for most Aleutian sites and >5 Hz for most mainland sites. Pink shadings indicate waveform segments used to locate individual tremor sources. Tremor observations at both sweet spots triggered by waves from the (a) *M*8.6 Sumatra, (b) Tohoku, (c) 2007 Kuril Islands earthquakes, (d) Queen Charlotte, (e) Chile, and (f) 2006 Kuril Islands earthquakes (Table 1).

### 3. Triggered Tremor

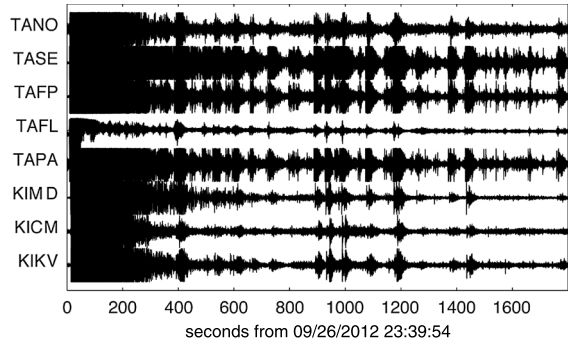
#### 3.1. Tremor Record Sections

[10] Out of the 11 candidate triggering wavefields studied, we observed triggered tremor for four cases in data recorded on the islands of Akutan, Unalaska, and several nearby islands and for five cases at sites on the mainland, most clearly in central Alaska (Tables 2 and 3). Figure 2 shows

record sections of the recorded, filtered, and envelope waveforms containing these triggered tremor signals.

[11] In addition to the above clear cases of triggered tremor, for two of the candidate triggering earthquakes results are ambiguous (Figure 3). These earthquakes occurred along the Aleutian arc within our study region so that the close proximity exposed the regions in their immediate vicinities to the largest amplitudes of all 11 candidate wave trains,

## (a) Andreanof Islands, Alndreanof Islands



## (b) Fox Islands, Akutan

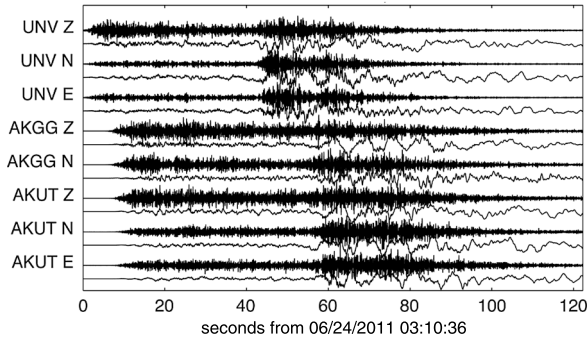


**Figure 3.** Record sections of waveforms including/following the two Aleutian candidate triggering earthquakes. Potential signals are difficult or impossible to discriminate from triggering source energy. (a) Vertical components waveforms filtered in the 2–10 Hz passband recorded at the networks nearest the epicenter of the Andreanof Islands earthquake (Table 1) show numerous aftershocks. (b) Three-component waveforms for the Fox Islands earthquake (Table 1) from stations on Akutan island as recorded on broadband sensors (lower traces) and after 2–10 Hz band-pass filtering (upper traces) show bursts of high-frequency energy arriving with the surface waves. See text.

at least at high frequencies (see section 4). In both cases all we can conclude is that tremor may have been triggered but was buried within energy carried in the *S* wave and *S* wave coda of the triggering waves. Tremor cannot be searched for at the stations near the Andreanof Islands earthquake because most data are clipped and show an almost continuous string of aftershocks (Figure 3a). At Aleutian stations where data are not clipped, energy in the 1–10 Hz tremor passband is observed during the passage of the *S* and Love waves, but it does not appear modulated, even within the Unalaska/Akutan sweet spot. Most of the seismograms of the larger and closer Fox Island earthquake were clipped at stations west of mainland Alaska, and where not clipped, if any tremor was triggered, it was buried within the energy carried in the *S* wave and its coda (Figure 3b). No tremor was observed at mainland sites for either of these candidate triggering earthquake wavefields.

### 3.2. Tremor Locations

[12] As the record sections in Figure 2 illustrate, the tremor signals often are just above the background noise level and, in a few cases, may be seen at spatially isolated stations so

that the criterion for being coherent at multiple stations cannot be evaluated. In addition, signals that likely radiated from local, background earthquakes also can be seen (e.g., during the wave trains at station BGL during the 2007 Kuril Islands earthquake and at stations RND and SAW during the Chile event in Figure 2). We also found that the ability to illuminate the tremor occasionally depended strongly on the filtering passband; in general, 2–10 Hz yielded more detections for the Aleutian data and >5 Hz for the mainland data.

[13] To locate the tremor sources, we applied the algorithm described in *Wech and Creager [2008]*, with windowed tremor signals. Given the subtlety of the tremor observations, we subjectively selected segments of the tremor signals with relatively higher signal-to-noise ratios and that appeared coherent across multiple stations (Figure 2). If nearly identical locations resulted for two contiguous segments, we combined them. The *Wech and Creager [2008]* algorithm is based on the cross correlation of envelope waveforms, and final locations included only waveforms that exceeded a correlation coefficient of >0.5. Although low relative to the criteria used in other studies, increasing a higher-correlation criterion often resulted in too few data to estimate a location. Hypocenters are estimated in the *Wech and Creager [2008]* method by performing a grid search over trial hypocenters, with the one that predicts phase lags that maximize the correlation considered most likely. We concluded that the depth estimates were not meaningful, verified by restricting the depth range of our grid in various intervals and finding the epicenter did not change. For the Aleutians, observations from multiple islands were required to obtain any location, which is not surprising given the much smaller intra-island station spacing relative to the distances to the likely tremor sources.

[14] All the tremor epicenters concentrate in two clusters, or sweet spots, despite the 6 year time interval. The Aleutian spot is centered between the islands of Unalaska and Akutan (Figure 4), centered on the 60 km plate-interface depth contours, and surrounding the distribution of ambient tremor source epicenters estimated in *Brown et al. [2013]*. *Chao et al. [2013]* also located the sources of multiple tremor bursts modulated by the Tohoku earthquake surface waves and found most in this same region. The one exception is a single burst that locates beneath the Shishaldin volcanic island just to the east of Akutan; its identification as tremor may be questioned given that tiny earthquakes are common there and modulation cannot be confirmed with just a single burst. The mainland tremor sources concentrate in a surprisingly small area, relative to the area over which the tremor was observed (Figure 5). This provides some confidence that while poorly constrained, the true epicenters probably all lie within the area bounded by stations PAX, DHY, SCM, and KLU. We discuss the relationships of these tremor sources to the regional tectonics in section 6.

### 4. Role of Candidate Triggering Deformations

[15] The probability of triggering tremor undoubtedly depends on both the characteristics of the candidate triggering deformation and the environment surrounding the tremor source. In this section we examine the former to assess whether a set of triggering characteristics can be distinguished from others that play little role in triggering tremor.

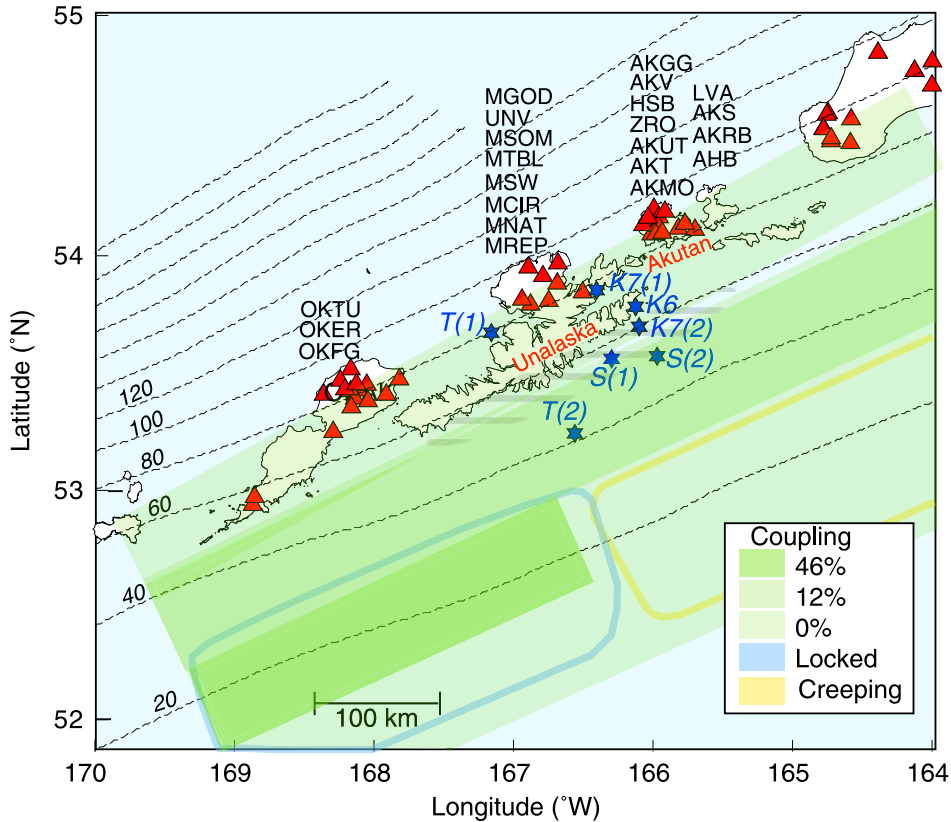


**Figure 4.** Map of epicenters of Unalaska/Akutan tremor sources. Tremor epicenters (blue stars) locate above where the plate-coupling transitions downdip from slightly coupled (12% interseismic slip deficit) to decoupled (0% slip deficit) according to the models of *Cross and Freymueller [2008]* (green shaded areas) and consistent with the more generalized coupling shown in *Freymueller et al. [2008]* (blue and yellow outlined areas). See text for more explanation. Seismic stations (red triangles) that provided data for locations are labeled (black lettering) as are the earthquake that radiated the waves that triggered the corresponding tremor source (blue lettering, abbreviations as in Figure 1). Numbers next to the latter indicating multiple sources were triggered, with waveform segments numbered identically in Figure 2. Contours (dashed) of the depth to the plate interface at 20 km intervals starting at the trench (numbers on left edge of map) are from *Hayes et al. [2012]*. Grey striped area shows where *Brown et al. [2013]* located ambient tremor sources.

[16] To do this, we measured features of vertical, radial, and tangential ( $Z$ ,  $R$ , and  $T$ ) component broadband velocities of the 11 candidate triggering wavefields studied, recorded at stations AKRB on Akutan Island and PAX on the mainland. Both these stations recorded most of the observed tremor signals. We show these waveforms at AKRB in Figure 6 and summarize the relevant features of these and of waveforms at PAX in Figure 7 and Tables 2 and 3. These features include the peak broadband velocities, back azimuths (calculated assuming propagation along a great-circle path on a spherical Earth), and the elapsed time since the previous triggered tremor.

[17] A number of studies have shown a correlation between the peak velocities of candidate triggering waves, which are proxies for peak strains [*Brune, 1970*], and the potential to trigger both earthquakes and tremor [*Miyazawa and Mori, 2006; Miyazawa and Brodsky, 2008; Peng et al., 2008, 2009, 2010; Ghosh et al., 2009; Rubinstein et al., 2009; Gomberg, 2010; Hill, 2010, 2012a, 2012b; Chao et al., 2012a, 2012b; Pollitz et al., 2012; Wu et al., 2012*]. The magnitudes of the triggering peak velocities we observe are

consistent with those in other studies, ranging from 0.04 to 0.4 cm/s or stresses of 4–40 kPa, assuming a rigidity of 40 GPa and shear velocity of 4 km/s [*Brune, 1970*]. The fact that such small stress changes appear to trigger tremor suggests that triggering occurs on near-failure faults. If the proximity to failure is key and we have observed failure of the same, or close fault patches, then triggered tremor should be more probable for longer elapsed time since the previous tremor event, assuming a steady stressing rate. We do not observe this, but note that we cannot rule out the possibility that tremor occurred between the candidate triggering earthquakes we studied or that the source faults are sufficiently close to one another. In fact, notes in AVO analysts' logs and the study of *Brown et al. [2013]* document episodes (lasting for tens of minutes to hours) of tremor activity near the Unalaska/Akutan sweet spot.

[18] We find an imperfect correlation between candidate triggering wave amplitude and triggering potential, if we consider only the peak velocity as a measure of the candidate triggering wavefield amplitude. The largest peak values correspond to triggered tremor observations for four of the five

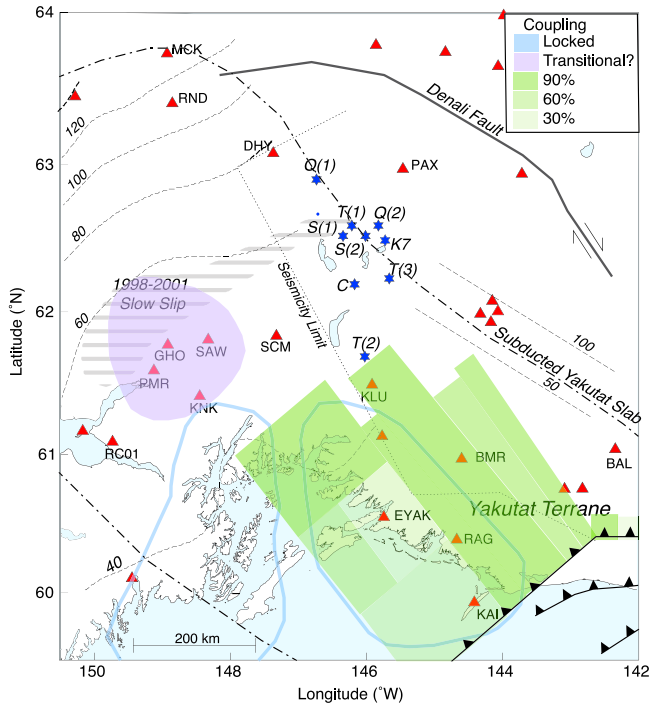


**Figure 5.** Map of epicenters of mainland tremor sources. Symbols and labels are the same as in Figure 4. Interseismic coupling between the Yakutat terrane and overlying Elias block estimated by *Elliott et al.* [2013] varies from 40% to 100% (light to darker green rectangle shading, respectively, with percent interseismic slip deficit), along a  $\sim 5^\circ$  northwest dipping plane. This interface coincides with but extends farther than the area estimated previously by *Freymueller et al.* [2008] (blue outlined kidney-shaped areas); note that the *Elliott et al.* [2013] study area is bounded by  $48^\circ\text{W}$  and  $62^\circ\text{N}$ . Hachured lines indicate thrust faults that accommodate Yakutat convergence. The triggered tremor sources locate outside the area above the 1998–2001 slow slip and tremor events (purple shading and grey stripes, respectively) [*Ohta et al.*, 2006; *Peterson and Christensen*, 2009], southwest of the Denali Fault zone, along the boundary of the subducted Yakutat slab inferred by *Eberhart-Phillips et al.* [2006] (dash-dotted curve), and where seismicity is relatively sparse (dotted line) [*Fuis et al.*, 2008]. The 50 and 100 km plate-interface contours (straight dashed lines) west of the tear are from *Page et al.* [1989].

triggering wavefields at the mainland PAX site and two of the four triggering wavefields at the Unalaska/Akutan site AKRB. In other words, nontriggering amplitudes exceed those of triggering wavefields in 20% and 50% of the observations of triggering for the mainland and Unalaska/Akutan sites, respectively.

[19] The imperfect correlations between peak amplitudes and triggered tremor led us to speculate that triggering requires exceeding amplitudes in a passband not captured by looking at peaks alone. We show spectral amplitudes at the Akutan site, AKRB (Figure 8). The spectral amplitudes of the triggering waves only exceed those of nontriggering waves at low frequencies (below  $\sim 0.03$  Hz), but notably in no single passband do all the triggering spectral amplitudes exceed those of the nontriggering signals. Several studies of

triggered tremor have suggested that triggering may be tuned to narrow passbands; e.g., *Miyazawa and Brodsky* [2008] infer that 0.3–0.07 Hz waves were more likely to trigger tremor in Japan than 0.025 Hz waves, and [*Peng et al.*, 2009] infer that waves in the 0.01–0.1 Hz passband facilitate triggering near Parkfield, California. Our observations lead us to conclude that while waves with frequencies below  $\sim 0.03$  Hz may facilitate triggering, frequency likely played a second-order role.

[20] The variability in the back azimuths provides a measure of the dependence of likelihood of Coulomb failure on the particular source fault geometry, because the Coulomb stresses imparted by Love and Rayleigh waves depend on the fault orientation and sense of slip [*Hill*, 2010, 2012a, 2012b]. At the Unalaska/Akutan site, the back azimuths for all the triggering waves cluster between  $267^\circ$  and  $280^\circ$  but range from  $122^\circ$  to  $300^\circ$  at the mainland site. The observations at the Unalaska/Akutan site may be generally consistent with Coulomb failure of sources along the plate interface, as incoming waves are approximately strike parallel and *Hill* [2010] shows that Love waves with approximately strike-parallel incidence promote Coulomb failure on low-angle reverse faults at 15–30 km depth (with the caveat that the plate interface dips more steeply and focal depths probably greater). Most of the tremor observations arrive during the Rayleigh waves visible in the broadband wave trains, but Love waves also arrive in the same windows. To unambiguously associate the tremor with Love waves requires that the tremor bursts arrive before the Rayleigh waves, but to ensure that this is the case, we would need to look in a variety of passbands because surface waves are dispersive (i.e., higher-velocity, lower frequency Rayleigh waves may not be visible without filtering broadband data). A precise correspondence between the tremor burst intervals and surface wave periods also would facilitate inference of the causative wave type. Both of these tests require correction for the different traveltimes between the tremor sources and stations of the tremor and surface waves. Such corrections were not attempted because in the best cases, we have only imprecise estimates of just the tremor source epicenters. For this reason and because there were very few relevant cases, we did not attempt to low-pass filter data to look for earlier arriving, lower frequency Rayleigh waves. We note however that Love wave triggering inferred from peak velocities alone is inconsistent with the observation that the peak tangential velocity from the nontriggering 2009 Kuril event exceeded that of the triggering 2007 Kuril earthquake waves. The variability in mainland back azimuths suggests the triggered source fault geometries varied and perhaps reflects the complex plate configuration in this part of Alaska.

## 5. Evidence for Slow Slip

[21] The lack of an obvious correlation between characteristics of the candidate triggering wavefields and occurrence of triggered tremor, previous inferences that ambient tremor is a proxy for slow slip [*Obara et al.*, 2004; *Aguiar et al.*, 2009], and several studies of triggered tremor that suggest triggering is more likely during slow slip events [*Rubinstein et al.*, 2009; *Gomberg*, 2010], led us to examine evidence for slow slip during the times when tremor was triggered in our study. Previous studies of GPS data from regions surrounding both

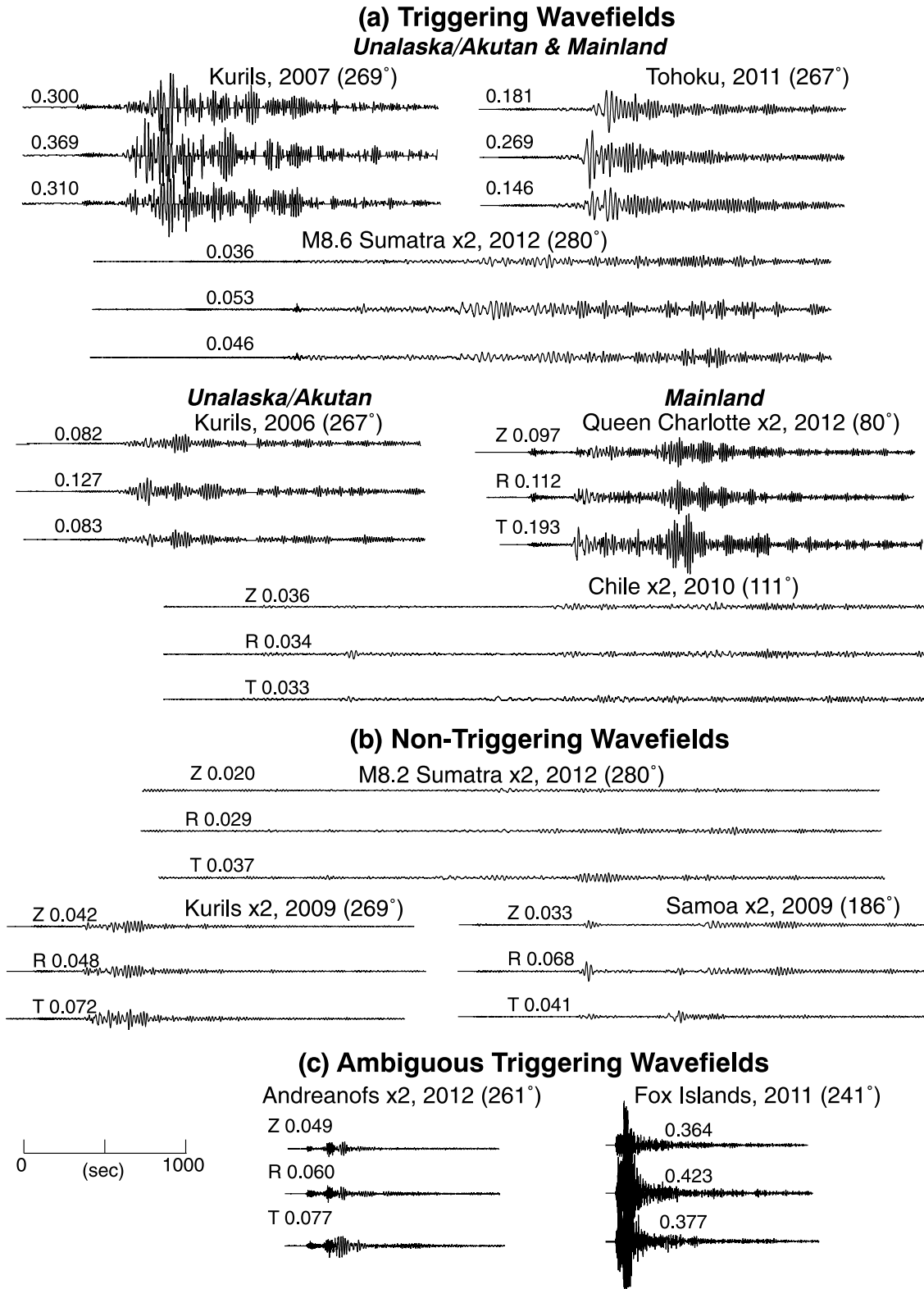


**Figure 6.** Candidate triggering wavefields. Velocity seismograms recorded at broadband station AKRB are plotted at the same scale except those with “x2” indicating amplitudes have been doubled for ease of visualization; numbers next to component labels are peak amplitudes in cm/s. Data are grouped according to the wavefields from events for which we (a) did or (b) did not identify triggered tremor or for which (c) the observations are unclear. The locations of where tremor was triggered are noted at the top. The back azimuths of the arriving waves are noted in parentheses. Table 1 lists triggering earthquake locations, origin times, and magnitudes.

Peak Velocities, Back-Azimuths, Triggering Status

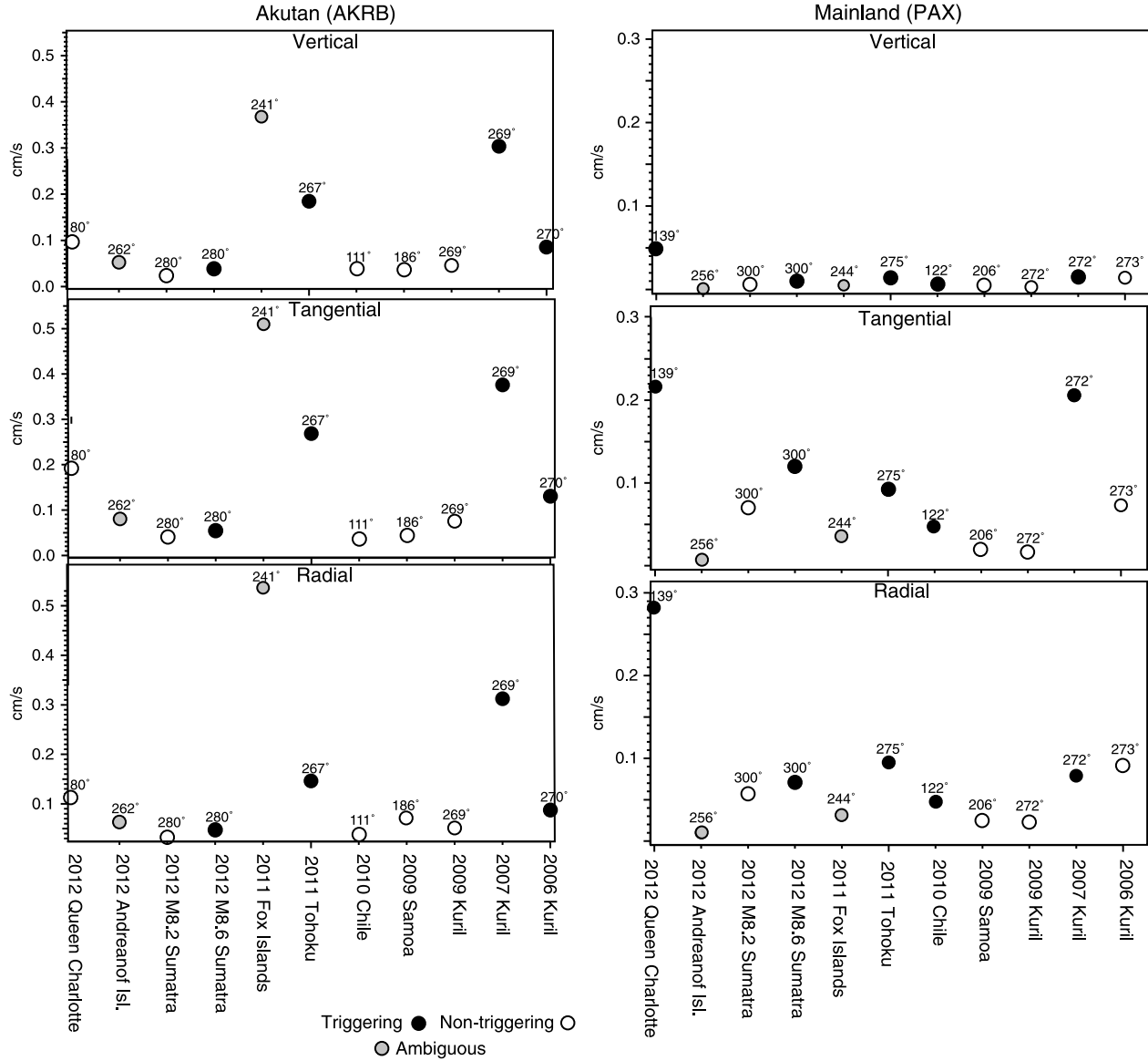


**Figure 7.** Summaries of candidate wavefield characteristics. Peak velocities ( $y$  axis) are plotted for each candidate triggering wavefield ( $x$  axis) with grey shading indicating whether the waves triggered tremor. Numbers above each circle denote back azimuths. These are measured from the waveforms in Figure 6, (left) at station AKRB on Akutan Island and (right) on the mainland at station PAX.

sweet spots provide negative evidence of slow slip correlating with triggered tremor (summarized below), but also some bound on the slip that may have occurred and gone undetected. *Peterson and Christensen* [2009] showed a few scattered tremor locations in the vicinity of the mainland sweet spot, but most located near the slow slip patch identified in *Ohta et al.* [2006] (Figure 5). We also visually examined GPS data processed somewhat differently than in previous studies, which confirmed the published results that evidence of slow slip is extremely subtle, if it exists at all.

[22] *Wei et al.* [2012] analyzed 2007–2011 GPS data in search of evidence of any slow slip events from an area that includes the mainland sweet spot (Figure 5) and the region surrounding Cook Inlet (see Figure 1) and found no evidence of slow slip beneath the sweet spot. Using a Network Strain

Filter analysis, they found coherent displacement changes of up to 5 mm on five GPS stations, beginning in early 2010 and continuing until the end of their data in late 2011. They modeled these displacements as a result of a maximum of 17 mm of slip on over a large area of the plate interface beneath Cook Inlet, with an equivalent magnitude of  $M6.9$ . The location of this event is over 100 km to the southwest of the 1998–2001 slow slip event described in *Ohta et al.* [2006] (Figures 1 and 5). Contrary to the aforementioned hypotheses that ambient tremor is a proxy for and triggered tremor more probable during slow slip events [*Obara et al.*, 2004; *Aguiar et al.*, 2009; *Gomberg*, 2010], none of the three candidate triggering wavefields that passed across the Cook Inlet during the slow slip event (Figure 9) triggered tremor, despite the Cook Inlet being relatively well monitored

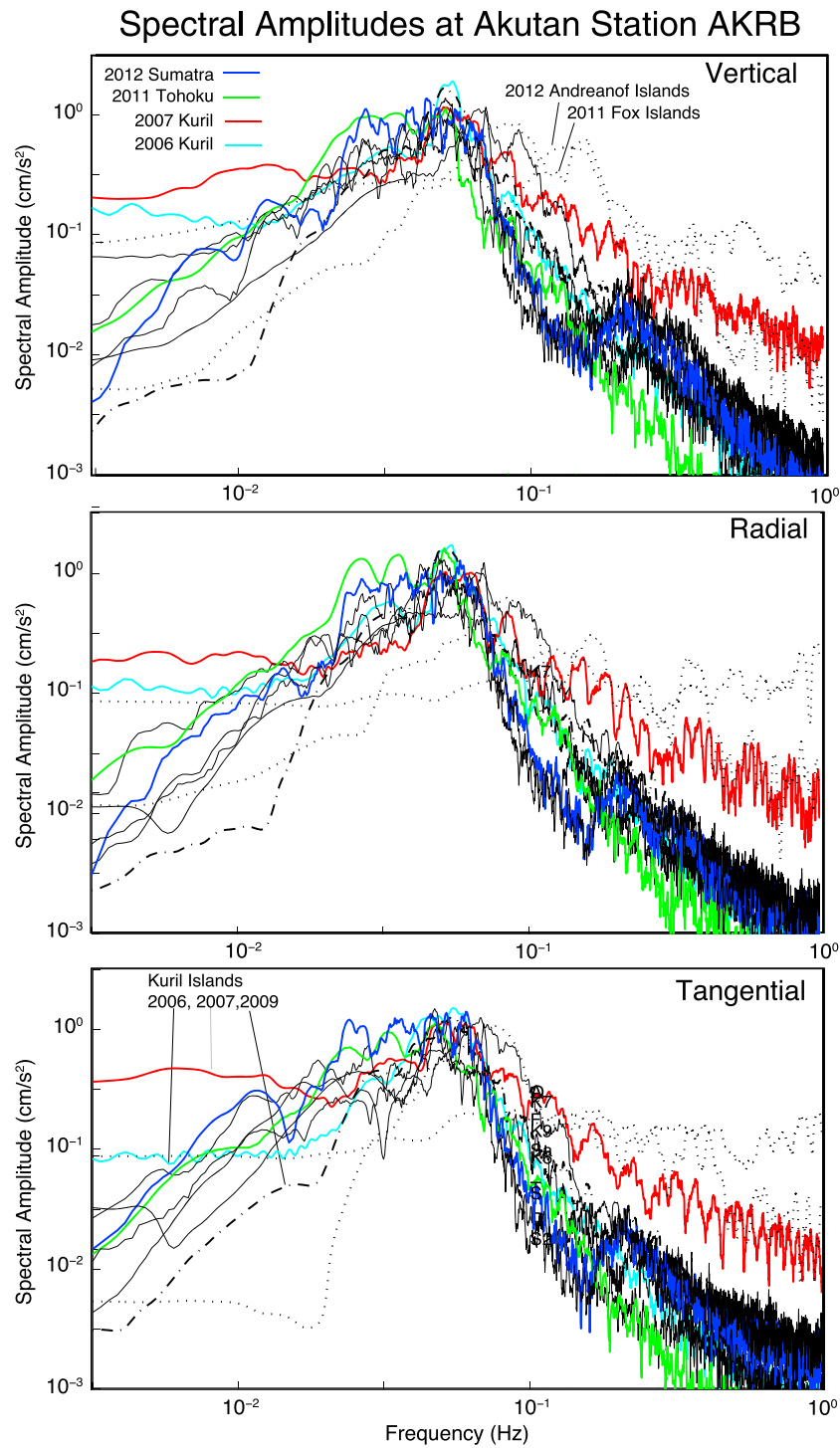


**Figure 8.** Amplitude spectra of candidate triggering waves. Spectral amplitudes (corrected for instrument sensitivity only) of all candidate triggering waves recorded at station AKRB on Akutan Island (shown in Figure 6); those that triggered tremor are shown by colored lines; red = 2007 Kuril, green = Tohoku, blue =  $M8.6$  Sumatra, cyan = 2006 Kuril. Dotted curves are spectra of waves for which triggering cannot be determined, from the Andeanof and Fox Islands earthquakes. Spectra of all remaining candidate triggering waves, for which no triggering was identified, are solid black curves except for those from the 2009 Kuril earthquake, shown as long dashed curves. See text for interpretations.

seismically and tremor being triggered by two wavefields in the mainland sweet spot. GPS data from Akutan Island from 2004 to early 2010 were studied by *Ji and Herring* [2011] who found a single deformation transient during the first half

of 2008, with maximum vertical and horizontal displacements of 9 mm and 11 mm, respectively. This signal was not apparent in the processed GPS data and only was identified using a principal component analysis. *Ji and Herring*

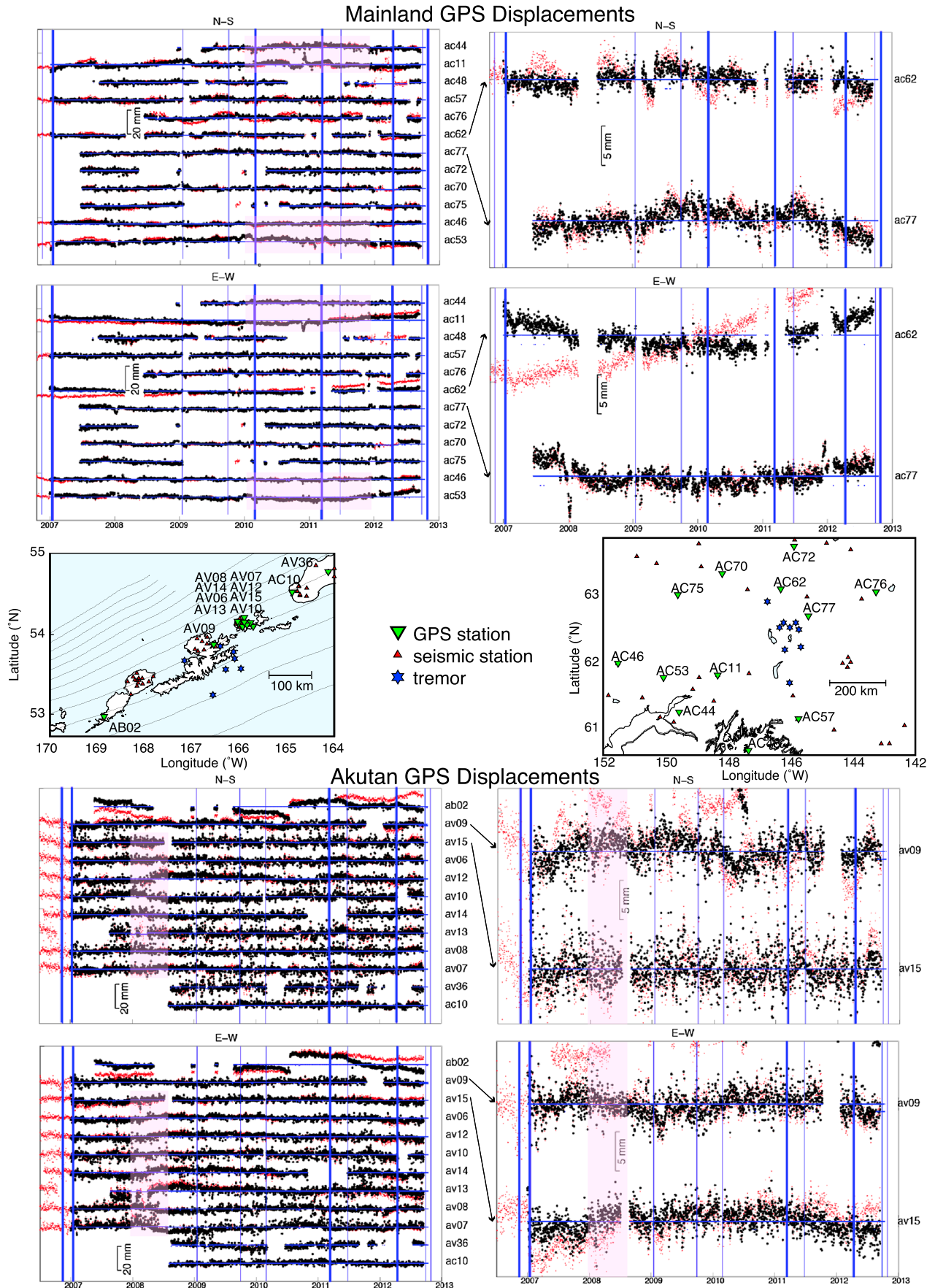


Figure 9

[2011] modeled the transient as a consequence of magma movement inside Akutan volcano.

[23] Figure 9 shows daily horizontal displacement estimates from GPS stations surrounding the mainland and Unalaska/Akutan sweet spots, derived and distributed by the Scripps Orbit and Permanent Array Center (SOPAC). The raw data position estimates have been corrected for common mode, annual and semiannual noise, a trend, and statistical outliers using parameters estimated by SOPAC (see <http://sopac.ucsd.edu/processing/refinedModelDoc.html> for descriptions of the estimation procedures). In addition, daily signal-to-noise ratio (SNR) estimates provided by the University NAVSTAR Consortium have been analyzed by K. Larson (personal communication, 2012) to determine thresholds for further elimination of poor-quality positions. This quality filtering is based on the fact that GPS instrumental noise generally is greatest in summer (due to warmer temperatures and higher thermal noise) and therefore average summer SNRs provide conservative thresholds for identifying outliers. That is, signals with SNR estimates lower than these thresholds, most likely resulting from snow-covering antennas, are assumed unreliable and removed. Although the seasonal variations in most of the Aleutians are not as great as in continental settings, this analysis did result in removal of months of data at a few sites, but otherwise did not significantly reduce the number of data. After removing unreliable data, annual signals and trends still were apparent so we fit and removed another set of trends and annual and semiannual sine waves (commonly done in GPS processing), justified perhaps because such variations likely arise from multiple sources with different phases. The Aleutian data are considerably noisier than those from mainland sites, perhaps reflecting the more volatile Aleutian climatic conditions. Examination of these “cleaned” data from the stations and time intervals in which *Wei et al.* [2012] and *Ji and Herring* [2011] inferred signals indicative of tectonic deformation confirms the conclusions from both those studies. That is, manifestations of any additional deformation in the vicinity of these stations in GPS data are difficult to distinguish with just visual examination of daily positions, even after attempts to remove the dominant noise.

[24] The slow slip inferred in *Wei et al.* [2012] and lack of clear differences in GPS signals during intervals when tremor was and was not triggered provide a very loose upper bound on any slow slip that might have facilitated tremor triggering on the plate interface. The patch of the plate interface where *Wei et al.* [2012] inferred the 2010–2011 slow slip event spans depth contours of 35–85 km. We infer that if of similar spatial and temporal wavelengths, then the maximum plate-interface slip would need to be less than a few centimeters to remain hidden.

## 6. Discussion

[25] Although our 6 year study period is very short geologically, we speculate that the prevalence of triggered tremor in the sweet spots over this period and the lack of correlation between triggering and any single characteristic of the triggering deformations indicate some properties of the tectonic environments make them conducive to tremor generation. We suggest that such proclivity is related to where the strength and frictional properties of the plate interface change, and additionally that these changes may mark the transitions between seismogenic and creeping regions. Longevity in such features also has been inferred from a correlation between present zones of slip deficit measured geodetically with past zones of high slip in earthquakes [*Frey Mueller et al.*, 2008].

[26] The plate configuration beneath central mainland Alaska is complex and uncertain, particularly in the region of the tremor sweet spot. South of the Denali Fault Zone, oceanic and arc terranes were transported and accreted to the North American plate, of which the Yakutat terrane is the most recent [*Plafker et al.*, 1994]. The Yakutat terrane is both colliding into and subducting beneath the Elias block of the southern Alaska margin [e.g., *Chapman et al.* [2008]; *Elliott et al.* [2013]]. As a result of this, deformation extends far into interior Alaska [*Haeussler*, 2008, AGU monograph 179]. In the collision zone, the north-northwestward directed collision of the Yakutat block with the region to the north gives rise to this complexity, with convergence changing northwestward from folding and thrusting to shallow subduction, with an abrupt transition between the two regimes [*Elliott et al.*, 2013]. Where subducting, the Yakutat terrane overlies the Pacific plate [*Brocher et al.*, 1994; *Frey Mueller et al.*, 2008], although more recent work suggests the entire thickness may be Yakutat terrane [*Christenson et al.*, 2010; *Worthington et al.*, 2012]. The Yakutat-North American plate (or Elias block) interface likely ruptured during the great 1964 M9.2 Alaska earthquake [*Eberhart-Phillips et al.*, 2006; *Frey Mueller et al.*, 2008], consistent with recent block modeling of high-resolution GPS data by *Elliott et al.* [2013], who inferred the interseismic coupling along the subducted Yakutat terrane interface to be spatially variable but strongly coupled over an area extending beyond the 1964 rupture (Figure 5). The tremor sweet spot lies at the approximate boundary of the subducted Yakutat slab inferred by *Eberhart-Phillips et al.* [2006] and just north of where the Yakutat-Elias block interface is strongly coupled [*Elliott et al.*, 2013], although it should be noted that the GPS data and study area of *Elliott et al.* [2013] also terminate just beyond the interface.

[27] In the region of the mainland sweet spot, *Fuis et al.* [2008] also infer that a “tear” may exist in part of the subducting

**Figure 9.** Daily horizontal ground displacements. Time series show horizontal displacements estimated from GPS signals (top and bottom) at stations (labeled) surrounding mainland (right map) and Unalaska/Akutan Island (left map) tremor epicenters, respectively. (left) All 11 stations’ data and (right) the two from the closest stations to the tremor. Raw data (red dots) are from the Scripps Orbit and Permanent Array Center and have been corrected for Center-determined common mode noise, annual and semiannual noise, a trend, and statistical outliers, and then for another fit annual and semiannual sine wave and trend (black dots). When raw signal-to-noise ratios were below a threshold, data have been omitted, such as in much of 2012 at station ac48 (Larson, personal communication, 2012). Pink vertical bands highlight data from stations and times where/when signals indicative of tectonic deformation were inferred from more sophisticated analyses [*Wei et al.*, 2012; *Ji and Herring*, 2011]. Vertical blue lines indicate dates candidate triggering waves passed each site, and thicker lines indicate triggering waves.

Pacific plate and note an abrupt and marked decrease in the seismicity rates from west to east at the western edge of the tremor distribution (Figure 5). (*Eberhart-Phillips et al.* [2006] find no evidence of this tear but cannot rule it out either.) Partly because of the paucity of seismicity, the precise configuration of the plate interface(s) beneath the tremor sweet spot is poorly constrained (e.g., the contours from *Hayes et al.* [2012] end just west of the tremor), although *Page et al.* [1989] infer 50 and 100 km interface contours east of the tremor based on sparse, probably uncertain hypocenters of inferred Benioff Zone earthquakes (Figure 5). The boundary of the subducted Yakutat slab inferred by *Eberhart-Phillips et al.* [2006], the areal extent of the coupled Yakutat terrane inferred in *Elliott et al.* [2013], and the relative lack of earthquake activity in the sweet spot region (Figure 5) are at least consistent with models in which tremor serves as a proxy for slow slip along an interface with frictional properties transitional between stable and stick-slip responses to tectonic loading. Future studies that provide more accurate tremor source locations, particularly their depths would be key in understanding the plate interactions and evolution in this region.

[28] The Unalaska/Akutan sweet spot is consistent with previous explanations of tremor and slow slip reflecting frictional properties that are transitional between those predicting stick-slip (seismogenic) and stable-sliding (creep) responses to loading [see *Rubin*, 2011, and references therein]. The Unalaska/Akutan tremor locates at the downdip transition, and we speculate at a lateral transition as well, as suggested from examples of ambient tremor globally [*Dragert et al.*, 2001; *Larson et al.*, 2004; *Ohta et al.*, 2004, 2006; *Wallace and Beavan*, 2010]. Figure 4 shows the tremor epicenters superposed on mapped projections of the more detailed and generalized coupling models from the studies of interseismic GPS data by *Cross and Freymueller* [2008] and *Freymueller et al.* [2008], respectively. Coupling in the former is represented as the percent interseismic slip deficit. Estimates of the 1957 M8.6 rupture plane cover the two coupled regions of the *Cross and Freymueller* [2008] model, apparently having slipped only at depth beneath the shallow decoupled zone in the eastern half of the region [*Cross and Freymueller*, 2008]. Interestingly, the tremor epicenters cluster at the roughly the same location along strike where the shallow coupling transitions laterally from decoupled to more strongly coupled. We speculate that the transitional nature of the interface extends downdip to where the tremor may originate. In other words, the transitional properties span a broader area (laterally and downdip) than in most places, possibly explaining its relatively high proclivity for both triggered and ambient tremor. This would imply that sweet spot also should exist at other lateral transition zones, such as at the edges of the Shumagin gap; indeed the eastern edge, with the most sharply defined transition, is one of the four regions in which *Peterson et al.* [2011] and *Brown et al.* [2013] identified ambient tremor. A gap in station coverage and a higher detection threshold in this same area may explain our failure to observe triggered tremor there.

## 7. Conclusions

[29] A search throughout Alaska reveals two tremor sweet spots—regions where large-amplitude seismic waves have repeatedly triggered tremor over a 6 year interval. While we examined all seismic network data throughout Alaska, we

cannot say definitively whether other such spots exist but are not detectable, given that tremor signals often are close to the detection thresholds throughout this huge and varied region [*D'Alessandro and Ruppert*, 2012]. Nonetheless, we can conclude that the probability of triggering tremor appears enhanced as triggering wave amplitudes increase and perhaps for lower frequencies, but neither these wave characteristics nor the geometric relationship of the wavefield to the tremor source faults alone ensures a high probability of triggering. The two sweet spots occur in tectonically very different subduction zone environments, indicating, for example, that age of the subducting plate or convergence rate does not determine the probability of triggering tremor. Contrary to previous evidence that ambient and triggered tremor are strong indicators of concurrent slow slip [*Obara et al.*, 2004; *Aguiar et al.*, 2009; *Gomberg*, 2010], we do not observe triggered tremor where and when slow slip has been documented.

[30] The failure to associate a single characteristic of the candidate triggering wavefield or of a permanent feature of the tectonic environment with a high or low probability of triggering suggested that perhaps transient plate-interface slip facilitated triggering. The occurrence of triggered tremor at the two sweet spots also does not correspond to times of visually detectable slow slip events but still permits the possibility that slow slip facilitated tremor triggering. If true, such slow slip events likely had to have lasted less than several months (time between triggering and nontriggering events), had dimensions of less than ~500 km (the approximate length of the mainland tremor sweet spot), and slipped less than several tens of centimeters if on the plate interface.

[31] The tremor sweet spot in the Aleutians, near the islands of Unalaska and Akutan, corroborates anecdotal evidence of common ambient tremor observed during routine visual scanning for volcano monitoring and results of the formal ambient tremor study of *Peterson et al.* [2011] and *Brown et al.* [2013]. A high probability of tremor occurring in this region perhaps should not be surprising given its coincidence with plate-interface frictional properties that are transitional between stick-slip (locked) and stably sliding (creeping), not just in the dip direction as observed elsewhere, but also laterally. Finding persistent tremor in mainland Alaska where no slow slip events have been detected was a surprise. Our triggered tremor observations suggest that additional studies looking for ambient tremor in this sweet spot would be fruitful, and if location estimates could be obtained, may provide new and useful constraints on the configuration and properties of the plate boundary in this complex region.

[32] **Acknowledgments.** The authors thank Aaron Wech for providing his tremor location codes and Kristine Larson for providing the results of her GPS signal-to-noise analyses. Data were recorded by the Alaska Earthquake Information Center, Alaska Volcano Observatory, Pacific and Alaska Tsunami Warning Centers, and Plate Boundary Observatory networks and distributed by the Incorporated Research Institutions for Seismology and the University Navstar Consortium. Kevin Chao, Julie Elliott, Justin Brown, Elizabeth Cochran, and Aaron Wech provided helpful reviews.

## References

- Aguiar, A. C., T. I. Melbourne, and C. W. Scrivner (2009), Moment release of Cascadia tremor constrained by GPS, *J. Geophys. Res.*, *114*, B00A05, doi:10.1029/2008JB005909.
- Ando, R., R. Nakata, and T. Hori (2010), A slip pulse model with fault heterogeneity for low-frequency earthquakes and tremor along plate interfaces, *Geophys. Res. Lett.*, *37*, L10310, doi:10.1029/2010GL043056.

- Brocher, T. M., G. S. Fuis, M. A. Fisher, G. Plafker, J. J. Taber, and N. I. Christensen (1994), Mapping the megathrust beneath the northern Gulf of Alaska using wide-angle seismic data, *J. Geophys. Res.*, *99*, 11,663–11,685.
- Brown, J. R., S. G. Prejean, G. C. Beroza, J. Gomberg, and P. J. Haeussler (2013), Deep low-frequency earthquakes in tectonic tremor along the Alaska-Aleutian subduction zone, *J. Geophys. Res. Solid Earth*, *118*, 1079–1090, doi:10.1029/2012JB009459.
- Brune, J. N. (1970), Tectonic stress and the spectra of seismic shear waves from earthquakes, *J. Geophys. Res.*, *75*, 4997–5009.
- Chao, K., Z. Peng, A. Fabian, and L. Ojha (2012a), Comparisons of triggered tremor in California, *Bull. Seismol. Soc. Am.*, *102*, 900–908.
- Chao, K., Z. Peng, C. Wu, C.-C. Tang, and C.-H. Lin (2012b), Remote triggering of non-volcanic tremor around Taiwan, *Geophys. J. Int.*, *188*(1), 301–324.
- Chao, K., Z. Peng, H. Gonzalez-Huizar, C. Aiken, B. Enescu, H. Kao, A. A. Velasco, K. Obara, and T. Matsuzawa (2013), A global search for triggered tremor following the 2011 *M<sub>w</sub>*9.0 Tohoku earthquake, *Bull. Seismol. Soc. Am.*, *103*(2b), 1551–1571, doi:10.1785/012012017.
- Chapman, J. B., et al. (2008), Neotectonics of the Yakutat collision: Changes in deformation driven by mass redistribution, in *AGU Geophys. Mono.*, vol. 179, edited by J. T. Freymueller et al., pp. 65–81, AGU, Washington, D.C.
- Christenson, G. L., S. P. S. Gulick, H. J. A. van Avendonk, L. L. Worthington, R. S. Reece, and T. L. Pavlis (2010), The Yakutat terrane: Dramatic change in crustal thickness across the Transition fault, Alaska, *Geology*, *38*(10), 895–898, doi:10.1130/G31170.1.
- Cross, R. S., and J. T. Freymueller (2008), Evidence for and implications of a Bering plate based on geodetic measurements from the Aleutians and western Alaska, *J. Geophys. Res.*, *113*, B07405, doi:10.1029/2007JB005136.
- D'Alessandro, A., and N. A. Ruppert (2012), Evaluation of location performance and magnitude of completeness of the Alaska Regional Seismic Network by the SNES method, *Bull. Seismol. Soc. Am.*, *102*, 2098–2115.
- DeMets, C., R. G. Gordon, D. F. Argus, and S. Stein (1994), Effect of recent revisions to the geomagnetic reversal timescale on estimates of current plate motions, *Geophys. Res. Lett.*, *21*, 2191–2194.
- Dixon, J. P., J. A. Power, and C. K. Searcy (2013), Catalog of earthquake hypocenters at Alaskan volcanoes: January 1 through December 31, 2011, U.S. Geological Survey Data Series 730, 82 p.
- Dragert, H., K. Wang, and T. James (2001), A silent slip event on the deeper Cascadia subduction interface, *Science*, *292*, 1525–1528, doi:10.1126/science.1060152.
- Eberhart-Phillips, D., D. H. Christensen, T. M. Brocher, R. Hansen, N. A. Ruppert, P. J. Haeussler, and G. A. Abers (2006), Imaging the transition from Aleutian subduction to Yakutat collision in central Alaska, with local earthquakes and active source data, *J. Geophys. Res.*, *111*, B11303, doi:10.1029/2005JB004240.
- Elliott, J., J. T. Freymueller, and C. F. Larsen (2013), Active tectonics of the St. Elias orogen, Alaska, observed with GPS measurements, *J. Geophys. Res. Solid Earth*, *118*, 5625–5642, doi:10.1002/jgrb.50341, in review.
- Freymueller, J. T. (2012), Observation of a “Locking Event”: A newly observed transient variation in the pattern of slip deficit at the Alaska Subduction Zone, *Seismol. Res. Lett.*, *83*, 433.
- Freymueller, J. T., S. C. Cohen, R. Cross, J. Elliott, H. J. Fletcher, S. Hreinsdottir, C. F. Larsen, and C. Zwick (2008), Active deformation processes in Alaska, based on 15 years of GPS measurements, in *AGU Geophys. Mono.*, vol. 179, edited by J. T. Freymueller et al., pp. 1–42, AGU, Washington, D.C.
- Fuis, G. S., et al. (2008), Trans-Alaska crustal transect and continental evolution involving subduction underplating and synchronous foreland thrusting, *Geology*, *36*, 267–270.
- Ghosh, A., J. E. Vidale, Z. Peng, K. C. Creager, and H. Houston (2009), Complex nonvolcanic tremor near Parkfield, California, triggered by the great 2004 Sumatra earthquake, *J. Geophys. Res.*, *114*, B00A15, doi:10.1029/2008JB006062.
- Ghosh, A., J. E. Vidale, and K. C. Creager (2012), Tremor asperities in the transition zone control evolution of slow earthquakes, *J. Geophys. Res.*, *117*, B10301, doi:10.1029/2012JB009249.
- Gomberg, J. (2010), Lessons from (triggered) tremor, *J. Geophys. Res.*, *115*, B10302, doi:10.1029/2009JB007011.
- Gomberg, J., S. Prejean, and N. Ruppert (2012), Afterslip, tremor, and the Denali Fault earthquake, *Bull. Seismol. Soc. Am.*, *102*, 892–899.
- Haeussler, P. J. (2008), An overview of the neotectonics of interior Alaska: Far-field deformation from the Yakutat Microplate collision, in *AGU Geophys. Mono.*, vol. 179, edited by J. T. Freymueller et al., pp. 83–108, AGU, Washington, D.C.
- Hayes, G. P., D. J. Wald, and R. L. Johnson (2012), Slab1.0: A three-dimensional model of global subduction zone geometries, *J. Geophys. Res.*, *117*, B01302, doi:10.1029/2011JB008524.
- Hill, D. P. (2010), Surface-wave potential for triggering tectonic (nonvolcanic) tremor, *Bull. Seismol. Soc. Am.*, *100*, 1859–1878.
- Hill, D. P. (2012a), Surface-wave potential for triggering tectonic (nonvolcanic) tremor—Corrected, *Bull. Seismol. Soc. Am.*, *102*, 2337–2355.
- Hill, D. P. (2012b), Erratum to dynamic stresses, Coulomb failure and remote triggering and to surface-wave potential for triggering tectonic (nonvolcanic) tremor, *Bull. Seismol. Soc. Am.*, *102*, 2795.
- Ji, K. H., and T. A. Herring (2011), Transient signal detection using GPS measurements: Transient inflation at Akutan volcano, Alaska, during early 2008, *Geophys. Res. Lett.*, *38*, L06307, doi:10.1029/2011GL046904.
- Koons, P. O., B. P. Hooks, T. Pavlis, P. Upton, and A. D. Barker (2010), Three-dimensional mechanics of Yakutat convergence in the southern Alaskan plate corner, *Tectonics*, *29*, TC4008, doi:10.1029/2009TC002463.
- Larson, K. M., V. Kostoglodov, A. Lowry, W. Hutton, O. Sanchez, K. Hudnut, and G. Suarez (2004), Crustal deformation measurements in Guerrero, Mexico, *J. Geophys. Res.*, *109*, B04409, doi:10.1029/2003JB002843.
- Miyazawa, M., and E. Brodsky (2008), Deep low-frequency tremor that correlates with passing surface waves, *J. Geophys. Res.*, *113*, B01307, doi:10.1029/2006JB004890.
- Miyazawa, M., and J. Mori (2006), Evidence suggesting fluid flow beneath Japan due to periodic seismic triggering from the 2004 Sumatra-Andaman earthquake, *Geophys. Res. Lett.*, *33*, L05303, doi:10.1029/2005GL025087.
- Obara, K. (2002), Nonvolcanic deep tremor associated with subduction in southwest Japan, *Science*, *296*(5573), 1679–1681, doi:10.1126/science.1070378.
- Obara, K., H. Hirose, F. Yamamizu, and K. Kasahara (2004), Episodic slow slip events accompanied by non-volcanic tremors in southwest Japan subduction zone, *Geophys. Res. Lett.*, *31*, L23602, doi:10.1029/2004GL020848.
- Ohta, Y., F. Kimata, and T. Sagiya (2004), Reexamination of the interplate coupling in the Tokai region, central Japan, based on the GPS data in 1997–2002, *Geophys. Res. Lett.*, *31*, L24604, doi:10.1029/2004GL021404.
- Ohta, Y., J. T. Freymueller, S. Hreinsdottir, and H. Suito (2006), A large slow slip event and the depth of the seismogenic zone in the south central Alaska subduction zone, *Earth Planet. Sci. Lett.*, *247*, 108–116.
- Page, R. A., D. S. Stephens, and J. C. Lahr (1989), Seismicity of the Wrangell and Aleutian Wadati-Benioff Zones and the North American Plate along the Trans-Alaska crustal transect, Chugach Mountains and Copper River Basin, southern Alaska, *J. Geophys. Res.*, *94*, 16,059–16,082.
- Peng, Z., and J. Gomberg (2010), An integrated perspective of the continuum between earthquakes and slow-slip phenomena, *Nat. Geosci.*, *22*, doi:10.1038/NNGEO940.
- Peng, Z., J. E. Vidale, K. C. Creager, J. L. Rubinstein, J. Gomberg, and P. Bodin (2008), Strong tremor near Parkfield, CA, excited by the 2002 Denali fault earthquake, *Geophys. Res. Lett.*, *35*, L23305, doi:10.1029/2008GL036080.
- Peng, Z., J. E. Vidale, A. G. Wech, R. M. Nadeau, and K. C. Creager (2009), Remote triggering of tremor along the San Andreas fault in central California, *J. Geophys. Res.*, *114*, B00A06, doi:10.1029/2008JB006049.
- Peng, Z., D. P. Hill, D. R. Shelly, and C. Aiken (2010), Remotely triggered microearthquakes and tremor in central California following the 2010 *M<sub>w</sub>* 8.8 Chile earthquake, *Geophys. Res. Lett.*, *37*, L24312, doi:10.1029/2010GL045462.
- Peterson, C. L., and D. H. Christensen (2009), Possible relationship between nonvolcanic tremor and the 1998–2001 slow slip event, south central Alaska, *J. Geophys. Res.*, *114*, B06302, doi:10.1029/2008JB006096.
- Peterson, C. L., S. R. McNutt, and D. H. Christensen (2011), Nonvolcanic tremor in the Aleutian Arc, *Bull. Seismol. Soc. Am.*, *101*, 3081–3087.
- Plafker, G., J. C. Moore, and G. R. Winkler (1994), Geology of the southern Alaska margin, in *The Geology of North America, Vol. G1, The Geology of Alaska*, edited by G. Plafker and H. C. Berg, pp. 389–449, Geol. Soc. Am., Boulder, Colo.
- Pollitz, F. F., R. S. Stein, and R. Burgmann (2012), The 11 April 2012 *M*=8.6 East Indian Ocean earthquake triggered large aftershocks worldwide, *Nature*, *490*, 250–253, doi:10.1038/nature11504.
- Rogers, G., and H. Dragert (2003), Episodic tremor and slip on the Cascadia subduction zone: The chatter of silent slip, *Science*, *300*(5627), 1942–1943, doi:10.1126/science.1084783.
- Rubin, A. M. (2011), Designer friction laws for bimodal slow slip propagation speeds, *Geochem. Geophys. Geosyst.*, *12*, Q04007, doi:10.1029/2010GC003386.
- Rubinstein, J. L., J. Gomberg, J. E. Vidale, A. G. Wech, H. Kao, K. C. Creager, and G. Rogers (2009), Seismic wave triggering of nonvolcanic tremor, episodic tremor and slip, and earthquakes on Vancouver Island, *J. Geophys. Res.*, *114*, B00A01, doi:10.1029/2008JB005875.
- Ruppert, N. A., J. M. Lees, and N. P. Kozyreva (2008), *Seismicity, Earthquakes and Structure Along the Aleutian and Kamchatka-Kurile Subduction Zones*, Geophys. Monograph Series 172, pp. 129–144, AGU, Washington, D.C.

## GOMBERG AND PREJEAN: TRIGGERED TREMOR SWEET SPOTS IN ALASKA

- Vidale, J. E., and H. Houston (2012), Slow slip: A new kind of earthquake, *Phys. Today*, 65(1), 38–43, doi:10.1063/PT.3.1399.
- Wallace, L. M., and J. Beavan (2010), Diverse slow slip behavior at the Hikurangi subduction margin, New Zealand, *J. Geophys. Res.*, 115, B12402, doi:10.1029/2010JB007717.
- Wech, A. G., and K. C. Creager (2008), Automated detection and location of Cascadia tremor, *Geophys. Res. Lett.*, 35, L20302, doi:10.1029/2008GL035458.
- Wech, A. G., and K. C. Creager (2011), A continuum of stress, strength and slip in the Cascadia subduction zone, *Nat. Geosci.*, 4, 624–628.
- Wei, M., J. J. McGuire, and E. Richardson (2012), A slow slip event in the south central Alaska subduction zone and related seismicity anomaly, *Geophys. Res. Lett.*, 39, L15309, doi:10.1029/2012GL052351.
- Worthington, L. L., H. J. A. Van Avendonk, S. P. S. Gulick, G. L. Christenson, and T. L. Pavlis (2012), Crustal structure of the Yakutat terrane and the evolution of subduction and collision in southern Alaska, *J. Geophys. Res.*, 117, B01102, doi:10.1029/2011JB008493.
- Wu, J., Z. Peng, W. Wang, X. Gong, Q. Chen, and C. Wu (2012), Comparisons of dynamic triggering near Beijing, China following recent large earthquakes in Sumatra, *Geophys. Res. Lett.*, 39, L21310, doi:10.1029/2012GL053515.

## GEOPHYSICS

## Tremor Sweet Spots

Seismic tremor is thought to be indicative of the slow release of small amounts of stress along plate boundaries, but it can also be triggered by large-amplitude seismic waves generated during large earthquakes. Gomberg and Prejean determined the distribution of tremor in Alaska after 11 of the largest earthquakes ( $M < 7.2$ ) around the globe between 2006 and 2012. As in previous observations, triggered tremor in the Aleutian Islands is related to the transition of friction along the subducting plate boundary from a locked state to a creeping state. How-

ever, tremor was also triggered in central mainland Alaska—a region far away from the subduction zone and devoid of any major crustal faults or appreciable seismic activity. Because there was no single characteristic of the triggering wave source or tectonic environment associated with the two regions, transient frictional processes at the plate interface may be responsible for tremor triggering. However, according to GPS data, neither zone shows any clear evidence of other concurrent related seismic processes such as slow slip events. — NW

*J. Geophys. Res.* **118**, 10.1002/2013JB010273 (2013).

## BIOCHEMISTRY

## Chirality Check

Most biological macromolecules are homochiral, and enzymes help to maintain this state of affairs; for example, checkpoints ensure that only L-amino acids are incorporated into proteins during translation. Among these enzymes is D-aminoacyl-tRNA deacylase (DTD), which removes D-amino acids mischarged onto tRNAs. Three types of DTDs have been identified, with the most common form being present in many bacteria and all eukaryotes. DTD faces the mech-

anism of acting on diverse D-aminoacyl-tRNAs (D-aa-tRNAs) while not harming L-aminoacyl-tRNAs (L-aa-tRNAs) that are present at much higher concentrations. Although crystal structures have been determined for DTD in the apo form and bound to free D-amino acids, the structural basis of enantioselectivity remained unclear. Ahmad *et al.* report the crystal structure of dimeric DTD from *Plasmodium falciparum* in complex with a substrate analog that mimics D-tyrosine attached to the 3'-OH of the terminal adenosine of tRNA. A critical role in shaping the active site for enantioselectivity is played by a Gly-cisPro motif that is inserted from one DTD monomer into the active site of the other monomer. Mainly main-chain atoms from DTD interact with the substrate, facilitating interaction with a range of D-aa-tRNAs. On the basis of mutational studies of active site residues, the authors suggest an RNA-assisted catalytic mechanism in which the RNA 2'-OH activates a water molecule. — VV

*eLife* **2**, e01519 (2013).

Thus, cells chronically exposed to excess glucose become less responsive to VEGF, which is necessary for the proper growth, function, and survival of endothelial cells. — LBR

*Sci. Signal.* **7**, ra1 (2014).

## CHEMISTRY

## As Thin As Clay Gets?

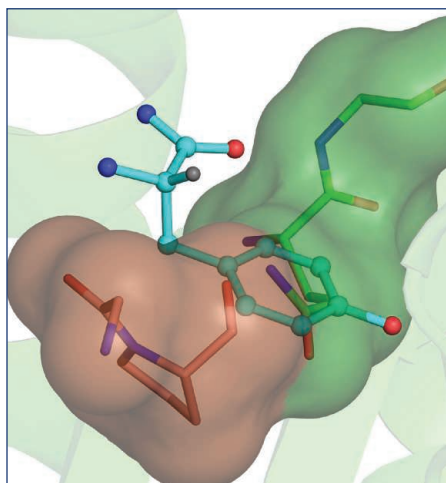
Thin films of aluminosilicates can mimic the reactivity of zeolites but avoid the kinetic limitations of diffusion through pore networks. Włodarczyk *et al.* build on their recent work on creating monolayers of aluminosilicates on the surfaces of single crystals of Ru to create thin films of Fe-containing silicates similar to the layers in smectite clays. Analysis of Si-O-Si stretching bands from infrared reflection-absorption spectroscopy revealed that the addition of Fe led to the formation of two-component films containing pure silica and an iron silicate. X-ray photoelectron spectroscopy (XPS) of an oxide with a 1:1 ratio of Fe to Si revealed a high coordination of O to Fe, and low-energy electron diffraction revealed greatly increased ordering even for small amounts of Fe incorporation. Density functional theory confirmed that uniform mixing of Fe is unfavorable thermodynamically as compared to phase separation, and favored a structure in which Fe atoms substitute for Si in the layer adjacent to the substrate and the formation of bridge Fe-O-Ru bonds. Although the Fe oxidation state could not be assigned from the XPS data, assuming that the Fe is in the 3+ oxidation state, the bilayer formed would represent a dehydroxylated form of nontronite, an Fe-rich smectite. — PDS

*J. Am. Soc. Chem.* **135**, 19222 (2013).

## CELL BIOLOGY

## Sugar Sabotage

In patients with diabetes, too much of a good thing—glucose—in the bloodstream causes the debilitating loss of biological functions and can eventually lead to death. Scientists continue to home in on the precise mechanisms by which this occurs, in hope of mitigating the damage. Warren *et al.* have found a mechanism by which excess glucose can alter the functions of vascular endothelial cells, one of the main sites of complications in diabetes. In mouse endothelial cells, too much glucose leads to the overproduction of reactive oxygen species (ROS) in the mitochondria. This excess of ROS causes the phosphorylation of the receptor for vascular endothelial growth factor (VEGF) within the Golgi, rendering the receptor vulnerable to proteolysis. This reduces the levels of VEGF receptor at the cell surface, where it would be able to detect circulating VEGF.



anism of acting on diverse D-aminoacyl-tRNAs (D-aa-tRNAs) while not harming L-aminoacyl-tRNAs (L-aa-tRNAs) that are present at much higher concentrations. Although crystal structures have been determined for DTD in the apo form and bound to free D-amino acids, the structural basis of enantioselectivity remained